A Histone Acetylation Switch Regulates H2A.Z Deposition by the SWR-C Remodeling Enzyme

Shinya Watanabe *et al.*

Science **340**, 195 (2013);
DOI: 10.1126/science.1229758

from their initial interactions with the monomer state (fig. S6). These data suggest that chaperone binding does not discriminate between folded and misfolded RNA states per se but that guanosine nucleotides are ultimately arranged in the final structure in such a way that chaperone binding (or inosine substitution) does not overly destabilize the final RNA structure. In this way, a guanosine-centric mechanism for RNA chaperone function is analogous to the mechanism of some chaperones that facilitate protein folding that destabilizes interactions involving hydrophobic amino acid residues (*21*). In these cases, both RNA and protein chaperones simply interact with residues especially prone to forming stable intermediate and non-native states.

References and Notes

1. D. Herschlag, *J. Biol. Chem.* **270**, 20871 (1995).
2. A. Rein, L. E. Henderson, J. G. Levin, *Trends Biochem. Sci.* **23**, 297 (1998).
3. L. Rajkowitsch *et al.*, *RNA Biol.* **4**, 118 (2007).
4. S. A. Woodson, *RNA Biol.* **7**, 677 (2010).
5. J. M. Coffin, S. H. Hughes, H. E. Varmus, *Retroviruses* (Cold Spring Harbor Press, Plainview, NY, 1997).
6. A. Rein, *RNA Biol.* **7**, 700 (2010).
7. J. A. Thomas, R. J. Gorelick, *Virus Res.* **134**, 39 (2008).
8. M. A. Adam, A. D. Miller, *J. Virol.* **62**, 3802 (1988).
9. C. S. Hibbert, J. Mirro, A. Rein, *J. Virol.* **78**, 10927 (2004).
10. C. Gherghe *et al.*, *Proc. Natl. Acad. Sci. U.S.A.* **107**, 19248 (2010).
11. C. S. Badorrek, K. M. Weeks, *Biochemistry* **45**, 12664 (2006).
12. C. Gherghe, C. W. Leonard, R. J. Gorelick, K. M. Weeks, *J. Virol.* **84**, 898 (2010).
13. S. A. Mortimer, K. M. Weeks, *J. Am. Chem. Soc.* **130**, 16178 (2008).
14. S. A. Mortimer, K. M. Weeks, *Nat. Protoc.* **4**, 1413 (2009).
15. P. T. Li, C. Bustamante, I. Tinoco Jr., *Proc. Natl. Acad. Sci. U.S.A.* **103**, 15847 (2006).
16. M. B. Eisen, P. T. Spellman, P. O. Brown, D. Botstein, *Proc. Natl. Acad. Sci. U.S.A.* **95**, 14863 (1998).
17. A. Dey, D. York, A. Smalls-Mantey, M. F. Summers, *Biochemistry* **44**, 3735 (2005).
18. D. J. Wright, J. L. Rice, D. M. Yanker, B. M. Znosko, *Biochemistry* **46**, 4625 (2007).
19. K. E. Deigan, T. W. Li, D. H. Mathews, K. M. Weeks, *Proc. Natl. Acad. Sci. U.S.A.* **106**, 97 (2009).
20. D. S. Portman, G. Dreyfuss, *EMBO J.* **13**, 213 (1994).
21. F. U. Hartl, M. Hayer-Hartl, *Nat. Struct. Mol. Biol.* **16**, 574 (2009).
22. T. Xia *et al.*, *Biochemistry* **37**, 14719 (1998).
23. J. Ding *et al.*, *Genes Dev.* **13**, 1102 (1999).

Acknowledgments: We are indebted to D. Grawoig for a critical review of the manuscript and to D. Johnson and C. Hixson for assistance in preparing MuLV NC protein. This work was supported by the U.S. National Institutes of Health (GM064803 to K.M.W., GM072518 to J.D.L., and GM031819 to Jack Griffith and B.D.B) and by the National Cancer Institute (under contract HHSN261200800001E with SAIC-Frederick, Inc. to R.J.G.). Data sets of representative clustered kinetic data are provided in the supplementary materials.

Supplementary Materials

www.sciencemag.org/cgi/content/full/science.1230715/DC1
Materials and Methods
Supplementary Text
Figs. S1 to S6
References (*24*–*32*)

25 September 2012; accepted 14 February 2013
Published online 7 March 2013;
10.1126/science.1230715

A Histone Acetylation Switch Regulates H2A.Z Deposition by the SWR-C Remodeling Enzyme

Shinya Watanabe,[1] Marta Radman-Livaja,[2] Oliver J. Rando,[2] Craig L. Peterson[1]*

The histone variant H2A.Z plays key roles in gene expression, DNA repair, and centromere function. H2A.Z deposition is controlled by SWR-C chromatin remodeling enzymes that catalyze the nucleosomal exchange of canonical H2A with H2A.Z. Here we report that acetylation of histone H3 on lysine 56 (H3-K56Ac) alters the substrate specificity of SWR-C, leading to promiscuous dimer exchange in which either H2A.Z or H2A can be exchanged from nucleosomes. This result was confirmed in vivo, where genome-wide analysis demonstrated widespread decreases in H2A.Z levels in yeast mutants with hyperacetylated H3K56. Our work also suggests that a conserved SWR-C subunit may function as a "lock" that prevents removal of H2A.Z from nucleosomes. Our study identifies a histone modification that regulates a chromatin remodeling reaction and provides insights into how histone variants and nucleosome turnover can be controlled by chromatin regulators.

The H2A.Z histone variant is typically found within nucleosomes that flank promoters of genes transcribed by RNA polymerase II, as well as nucleosomes that flank chromatin boundary elements, centromeres, and replication origins (*1*–*3*). These nucleosomes also exhibit rapid, replication-independent turnover, which is thought to function in erasing histone marks, preventing the spread of chromatin states, and ensuring general plasticity of the epigenome (*4*, *5*). H2A.Z appears to enhance rapid turnover of promoter proximal nucleosomes in yeast (*4*), and nucleosomes subject to rapid turnover kinetics are also enriched for histone H3 acetylated at lysine 56 (H3-K56Ac) (*6*). H3-K56Ac is also required for enhanced turnover of promoter nucleosomes (*6*, *7*). Recent work indicates that vertebrate gene promoters are also enriched in nucleosomes harboring both H2A.Z and H3-K56Ac, suggesting a conserved regulatory relationship (*2*, *8*, *9*). How they cooperate in this process, though, is not clear.

To test whether nucleosomes that harbor both H2A.Z and H3-K56Ac are inherently unstable, recombinant yeast mononucleosomes were immobilized on streptavidin beads, and nucleosome stability was monitored after exposure to increasing salt concentration (fig. S1). Nucleosomes were reconstituted with either H2A/H2B or H2A.Z/H2B dimers, and with histone H3 that contained either a lysine at position 56 or a glutamine residue to mimic acetylation (H3-K56Q). H3-K56Q had no detectable effect on the stability of the H2A/H2B dimer–H3/H4 tetramer interaction (fig. S1, top panels) (*10*, *11*). By contrast, incorporation of H2A.Z led to a decreased salt stability of both H3 and H3-K56Q mononucleosomes (fig. S1, bottom left panel) (*12*). However, the combination of H2A.Z and H3-K56Q did not further decrease stability (fig. S1, bottom right panel), indicating that this H3 modification does not itself contribute to marked instability of nucleosomes.

The conserved SWR-C chromatin remodeling enzyme controls H2A.Z deposition in yeast (*13*, *14*), and so we next tested whether H3-K56Ac might regulate its histone exchange activity. Recombinant yeast H2A mononucleosomes that harbored either H3-K56 or H3-K56Q were incubated with purified SWR-C, recombinant H2A.Z/H2B dimers, and adenosine 5′-triphosphate (ATP), and then histone exchange was quantified by a Western blot assay, probing for different epitope-tagged, H2A histones. The integrity of the mononucleosome was analyzed by both Western blotting for H3 and by visualizing DNA (Fig. 1). SWR-C catalyzed robust deposition of H2A.Z when incubated with the wild-type H2A nucleosomes (*14*). By contrast, nearly 80% less H2A.Z was deposited by SWR-C when incubated with the H3-K56Q substrate (Fig. 1A and fig. S2).

SWR-C–catalyzed dimer exchange involves at least two coupled steps—ATP-dependent eviction of the H2A/H2B dimer from the nucleosome, followed by deposition of H2A.Z/H2B (*15*). We predicted that H3-K56Ac might facilitate both the forward and reverse reactions and might display altered substrate specificity more like that of the related INO80 enzyme (*16*). We

[1]Program in Molecular Medicine, 373 Plantation Street, University of Massachusetts Medical School, Worcester, MA 01605, USA. [2]Department of Biochemistry and Molecular Pharmacology, 364 Plantation Street, University of Massachusetts Medical School, Worcester, MA 01605, USA.

*Corresponding author. E-mail: craig.peterson@umassmed.edu

incubated SWR-C with H2A.Z nucleosomes, ATP, and H2A/H2B dimers and found that SWR-C had no effect on the histone composition of the wild-type H2A.Z nucleosome, as expected (Fig. 1B) (*14*, *16*). By contrast, SWR-C showed robust eviction of nucleosomal H2A.Z when the nucleosome harbored H3-K56Q (Fig. 1B and fig. S3). Furthermore, SWR-C catalyzed the ATP-dependent incorporation of H2A when incubated with the H2A.Z/H3-K56Q mononucleosome (Fig. 1B). H2A.Z exchange was efficient, with nearly 30% H2A replacement (Fig. 1C). H3-K56Q also stimulated a low level of H2A.Z exchange in the absence of SWR-C, indicating that this modification may poise the H2A.Z nucleosome for exchange events (Fig. 1B), perhaps due to enhanced breathing of nucleosomal DNA (*11*). Robust H2A.Z exchange reaction was dependent on the concentration of SWR-C (fig. S3), ATP, and the time of incubation (fig. S4). H3-K56Q also enhanced the H2A.Z replacement activity of the related INO80 enzyme (Fig. 1B and fig. S5). These effects of H3-K56Q were not due to alterations in the nucleosome binding affinity of the SWR-C or INO80 enzymes (fig. S6). We further examined whether the alterations in SWR-C could also be observed with bona fide H3-K56Ac mononucleosomes (fig. S7) that were incubated with SWR-C in the presence of H2A/H2B dimers (Fig. 1D and fig. S8). SWR-C catalyzed the ATP-dependent incorporation of H2A, similar to our results with an H2A.Z nucleosome harboring H3-K56Q.

The substrate specificity of the SWR-C dimer-exchange reaction is reflected by the adenosine triphosphatase (ATPase) properties of SWR-C, as an H2A nucleosome, but not an H2A.Z nucleosome, stimulates the ATPase activity of SWR-C (*15*). Because ATP-dependent remodeling enzymes are DNA-stimulated ATPases, these results suggest that SWR-C productively interacts only with the nucleosomal DNA of an H2A nucleosome, consistent with the dimer exchange specificity of SWR-C. To determine if H3-K56Q alters the ATPase properties of SWR-C, ATPase assays were performed with wild-type and H3-K56Q nucleosomes. The ATPase activity of SWR-C was stimulated by an H2A nucleosome, but no stimulation was observed with the H2A.Z nucleosome (Fig. 2A). The addition of free H2A.Z/H2B dimers led to a further stimulation (*15*). By contrast, nucleosomal incorporation of H3-K56Q led to equal ATPase stimulation by both the H2A and H2A.Z nucleosomes, and addition of free dimers had no effect (Fig. 2B).

The Swc2p subunit of SWR-C binds to H2A.Z, and Swc2p is required for deposition of H2A.Z in vitro (*17*) and in vivo (*13*), suggesting that Swc2p functions during the H2A.Z deposition step of the dimer-exchange reaction, presumably by binding and delivering H2A.Z (*17*). We hypothesized that Swc2p might also function at the end of the reaction cycle, functioning as a molecular "lock" that binds to H2A.Z and prevents SWR-C from removing the newly incorporated H2A.Z.

SWR-C was purified from a *swc2*Δ strain, yielding a SWR-C that lacks the Swc2p and Swc3p subunits and was depleted for Arp6 and Swc6 (fig. S9). The Swc2Δ subcomplex was unable to deposit H2A.Z into an H2A nucleosome (fig. S10) (*17*), but it catalyzed the ATP-dependent eviction of H2A.Z and promoted H2A incorporation (Fig. 2C). Thus, the activity of the Swc2Δ subcomplex shows similarity to that of SWR-C

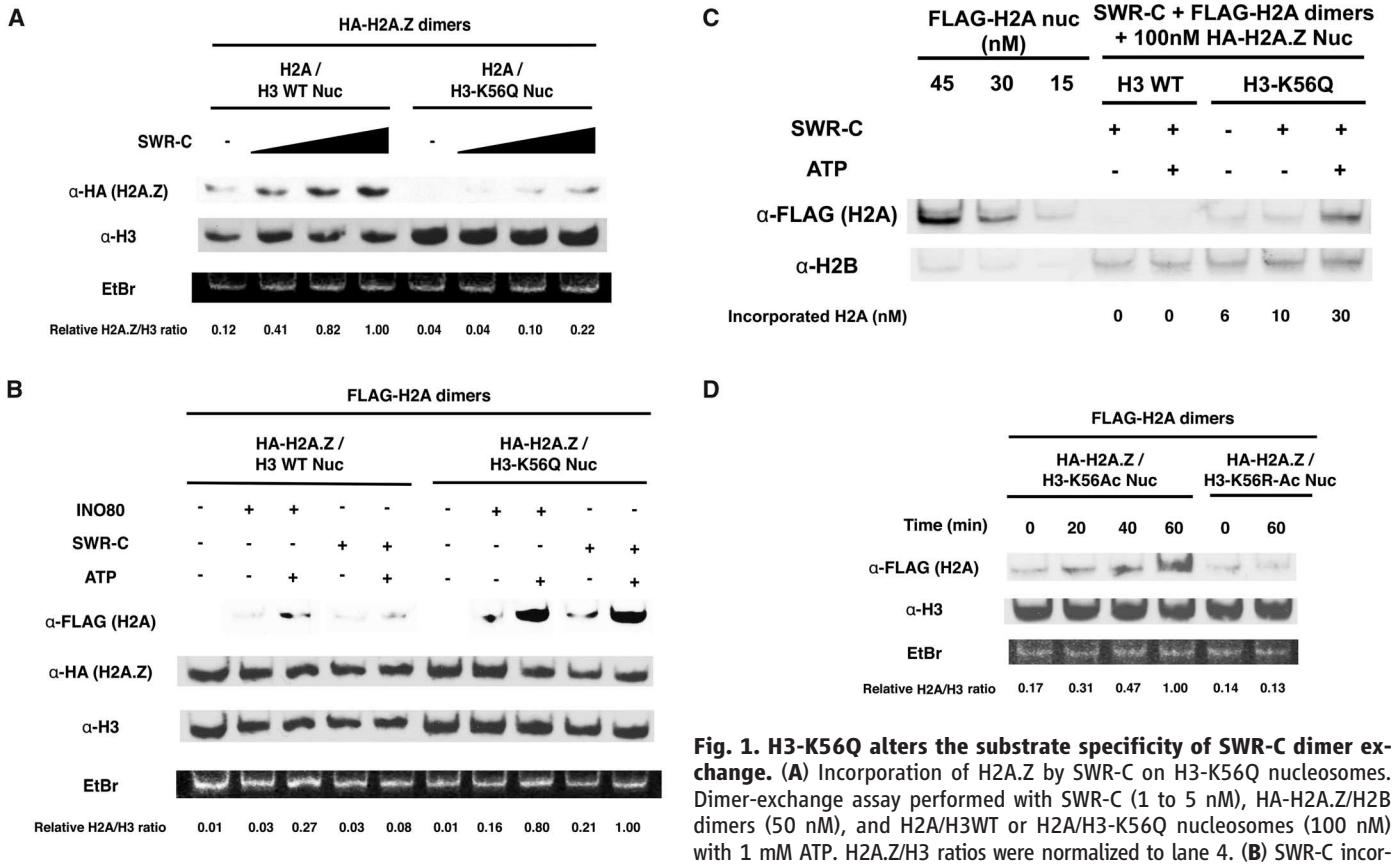

Fig. 1. H3-K56Q alters the substrate specificity of SWR-C dimer exchange. (**A**) Incorporation of H2A.Z by SWR-C on H3-K56Q nucleosomes. Dimer-exchange assay performed with SWR-C (1 to 5 nM), HA-H2A.Z/H2B dimers (50 nM), and H2A/H3WT or H2A/H3-K56Q nucleosomes (100 nM) with 1 mM ATP. H2A.Z/H3 ratios were normalized to lane 4. (**B**) SWR-C incorporates H2A into H2A.Z /H3-K56Q nucleosomes and H3-K56Q stimulates dimer-exchange activity of INO80. Dimer-exchange assay performed with 5 nM SWR-C or 1 nM INO80, FLAG-H2A/H2B dimers (50 nM), and HA-H2A.Z/H3WT or HA-H2A.Z/H3-K56Q nucleosomes (100 nM) with (+) or without (–) 1 mM ATP. Each H2A/H3 ratio was normalized to lane 10. (**C**) SWR-C–mediated deposition of H2A quantified by quantitative western blotting (LI-COR). Dimer-exchange assays performed with 10 nM SWR-C, FLAG-H2A/H2B dimer and NAP1 (200 nM), and HA-H2A.Z/H3WT or HA-H2A.Z /H3-K56Q nucleosomes (100 nM) with or without 1 mM ATP. (**D**) H3K56Ac stimulates H2A deposition by SWR-C. Dimer-exchange assay performed with SWR-C (5 nM), ATP (1 mM), FLAG-H2A/H2B dimers (50 nM), and HA-H2A.Z/H3-K56Ac or HA-H2A.Z/H3-K56R-Ac nucleosomes (100 nM) generated by in vitro acetylation with Rtt109/Vps75 acetyltransferase. EtBr, ethidium bromide.

with an H3-K56Q nucleosome. The ATPase activity of the Swc2Δ subcomplex was stimulated by an H2A.Z nucleosome, but not an H2A nucleosome, the opposite substrates compared to intact SWR-C (Fig. 2D). Thus, the Swc2/3 module appears to play a key role in substrate specificity, promoting activity on an H2A nucleosome and preventing the remodeling of an H2A.Z nucleosome. Swc2p binds to the C-terminal domain of H2A.Z that is near H3-K56 within the nucleosome; thus, we propose that H3-K56Ac might disrupt Swc2p function, allowing SWR-C to act on a H2A.Z nucleosome. Consistent with this view, the activity of the Swc2Δ subcomplex was not influenced by H3-K56Q (fig. S11).

Our model predicts that constitutive acetylation of H3-K56 in vivo should promote H2A.Z exchange, leading to decreased steady-state levels. To test this model, we carried out genome-wide mapping of H2A.Z in yeast with globally increased levels of H3K56Ac. For these analyses, yeast strains were used that either express H3K56Q, or lack the Hst3p and Hst4p deacetylases that target H3-K56Ac (*18*, *19*). In our wild-type control, we recapitulated the previously reported localization of H2A.Z (*1*, *3*), with maximal enrichment at genic +1 nucleosomes and more modest enrichment at the –1 nucleosome. Notably, in both strains carrying globally increased H3-K56ac, H2A.Z levels were on average diminished at promoters (Fig. 3A). *HTZ1* (H2A.Z) mRNA levels were unchanged in H3-K56Q and *hst3Δ/hst4Δ* strains (fig. S12). Because Fig. 3A shows an averaged view over all genes, we also sought to understand whether this loss of H2A.Z was universal or specific to a small subset of genes. As shown in Fig. 3, B and C, H2A.Z was generally lost from +1 nucleosomes—nucleosomes normally exhibiting modest or minimal enrichment of H2A.Z (H2A.Z levels in wild type from 0 to 3) were little affected by global hyperacetylation, whereas nucleosomes carrying higher amounts of H2A.Z almost universally lost H2A.Z in strains harboring constitutive H3-K56Ac (see also fig. S13). Consistent with the idea that H3K56Ac leads to SWR-C–dependent H2A.Z replacement, H2A.Z was lost in hyperacetylation mutants primarily at genes associated with SWR-C, whereas genes lacking SWR-C in prior mapping studies (*20*) were largely unaffected in these mutants (Fig. 3D and fig. S13C).

H2A.Z incorporation was also monitored in wild-type and H3-K56Q strains during the re-establishment of transcriptional repression at the *PHO5* gene. In both the wild-type and H3-K56Q strains, H3 levels were restored to similar extents when *PHO5* was repressed; however, H2A.Z was at least 50% less in the H3-K56Q strain (fig. S14). Finally, we tested whether the gene expression profiles of an H3-K56Q strain are similar to that of a strain that lacks H2A.Z. We observed a significant overlap in gene expression defects and a positive correlation between changes in mRNA levels between *htz1Δ* and H3K56Q strains (Fig. 4). These data are consistent with H3K56Ac modulating SWR-C dimer-exchange activity in vivo.

A functional connection between histone modifications and ATP-dependent remodeling enzymes has long been recognized (*21*). Here we find that H3-K56Ac (or H3-K56Q) functions as a switch that changes the remodeling specificity of the SWR-C dimer-exchange reaction, leading to removal of H2A.Z from the nucleosomal product. Our data indicate that Swc2p functions to prevent activation of the Swr1 ATPase by an H2A.Z nucleosome, and that it may function at the end of the reaction cycle to "lock" H2A.Z and prevent its eviction. Swc2p is conserved from yeast to human (*17*), and YL-1, the metazoan counterpart of Swc2p, is found in the *Drosophila* and human counterparts of SWR-C, the dTip60 and SRCAP complexes, respectively (*22*, *23*). Thus, it is likely that both the proposed "lock" function of Swc2 and the role of H3-K56Ac are conserved in higher eukaryotes. Our work suggests a model whereby an H3-K56Ac

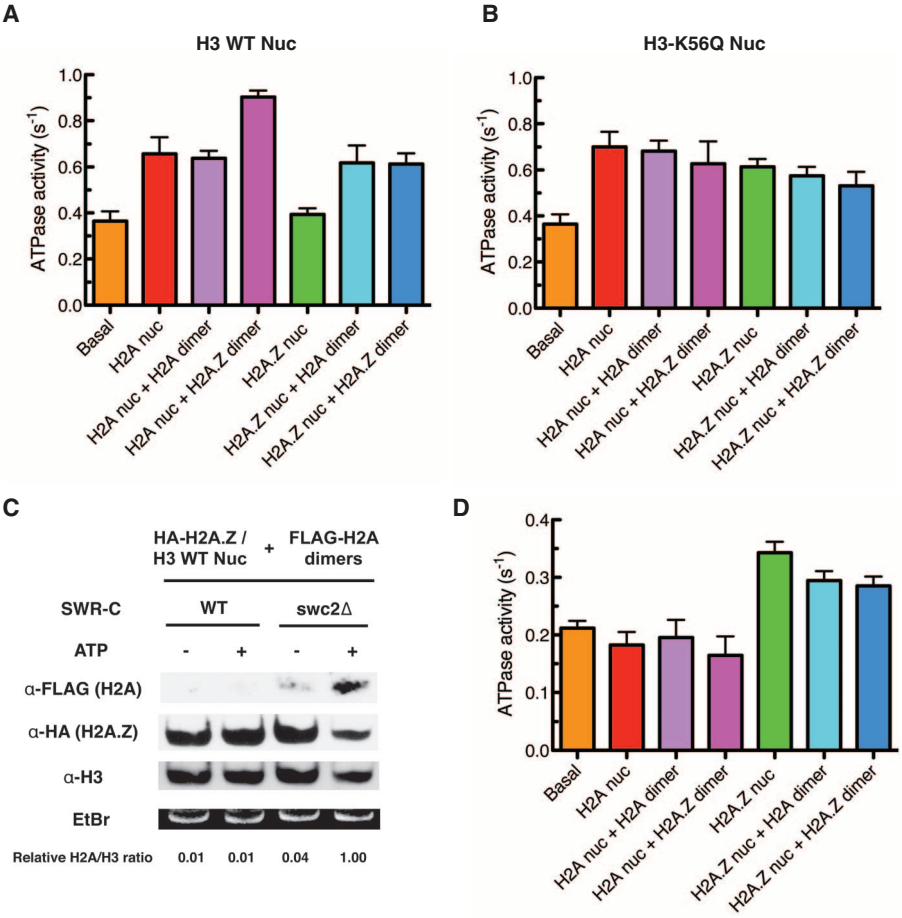

Fig. 2. Roles for H3-K56Q and Swc2p in modulating the ATPase cofactor requirements of SWR-C. (**A**) Substrate specificity of SWR-C ATPase activity on H3WT nucleosomes. SWR-C (1 nM) and 0.1 mM ATP was incubated with (+) or without (–) nucleosomes (15 nM) or free dimers (15 nM). ATPase assays measured fluorescent change of 7-diethylamino-3-({[(2-maleimidyl)-ethyl]amino}carbonyl)coumarin-labeled phosphate-binding protein (MDCC-PBP) upon phosphate binding. Data represent the results from three independent experiments and error bars reflect standard deviations. (**B**) Substrate specificity of ATPase activity of SWR-C on H3-K56Q nucleosomes. As in (A), but nucleosomes harbored H3-K56Q. (**C**) The Swc2Δ subcomplex exchanges H2A.Z with H2A. The dimer-exchange assay performed with 5 nM SWR-C WT or Swc2Δ subcomplex, FLAG-H2A/H2B dimers (50 nM), and HA-H2A.Z/H3WT nucleosomes (100 nM) with or without 1 mM ATP. Each H2A/H3 ratio was normalized to lane 4. EtBr, ethidium bromide. (**D**) Substrate specificity of the Swc2Δ subcomplex.

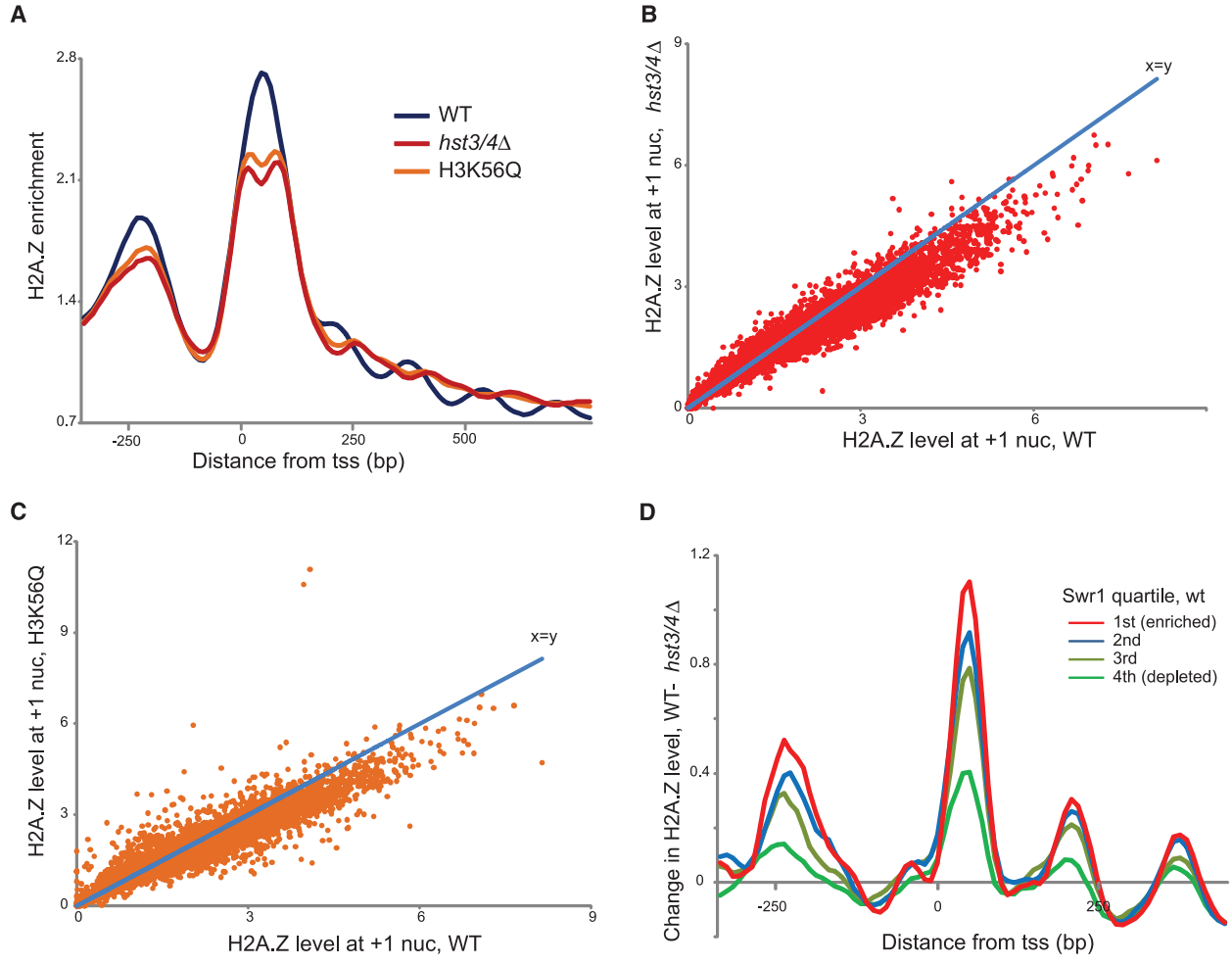

Fig. 3. Constitutive H3-K56Ac decreases steady-state levels of promoter-proximal H2A.Z in vivo. (**A**) H2A.Z enrichments at promoter regions in wild-type (WT) and H3-K56Q strains. Chromatin immunoprecipitation sequencing (ChIP-Seq) using antibody against H2A.Z in WT, *hst3*Δ *hst4*Δ, and H3K56Q strains. After alignment to the genome, normalized read counts were averaged for all genes aligned on the basis of their transcriptional start sites (TSS). (**B** and **C**) Scatterplot of H2A.Z levels at genic +1 nucleosomes for WT (*x* axis) versus either *hst3*Δ *hst4*Δ (B) or H3K56Q (C) mutants. Blue lines show $x = y$ line. The vast majority of genes exhibit a decrease in H2A.Z levels in either of the H3K56 hyperacetylated mutants. (**D**) H2A.Z loss preferentially occurs at genes associated with the SWR-C complex. Swr1 levels [from (*20*)] were calculated for all genes, and genes are grouped into four quartiles according to Swr1 abundance. Change in H2A.Z levels at the +1 nucleosome in WT and *hst3*Δ *hst4*Δ strains is shown at promoters, showing that genes with the lowest Swr1 levels exhibited lower changes in H2A.Z levels than remaining genes with moderate to high Swr1 levels.

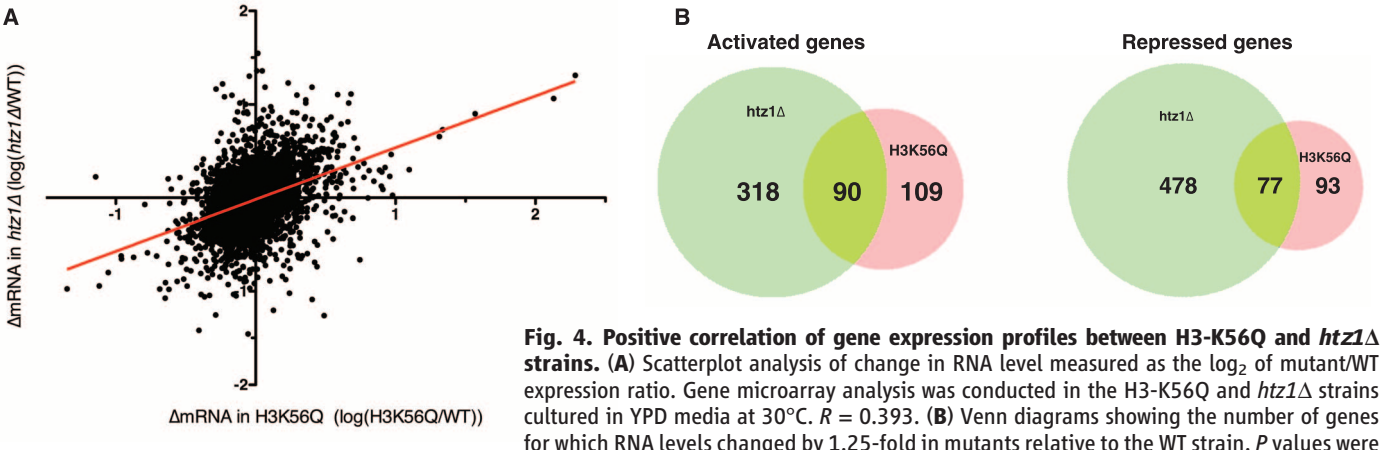

Fig. 4. Positive correlation of gene expression profiles between H3-K56Q and *htz1*Δ strains. (**A**) Scatterplot analysis of change in RNA level measured as the $\log_2$ of mutant/WT expression ratio. Gene microarray analysis was conducted in the H3-K56Q and *htz1*Δ strains cultured in YPD media at 30°C. $R = 0.393$. (**B**) Venn diagrams showing the number of genes for which RNA levels changed by 1.25-fold in mutants relative to the WT strain. *P* values were 8×10^{-54} (45% overlap in activated genes) and 9×10^{-36} (45% overlap in repressed genes).

nucleosome may be subject to multiple rounds of SWR-C–catalyzed dimer exchange and such promiscuous dimer exchange may promote subsequent histone H3/H4 turnover (fig. S15). This model provides a mechanistic explanation for how H3-K56Ac and H2A.Z might coordinately control nucleosome turnover at regulatory regions (*3*) by regulating the activity and substrate specificity of chromatin remodeling enzymes.

References and Notes

1. R. M. Raisner *et al.*, *Cell* **123**, 233 (2005).
2. A. Barski *et al.*, *Cell* **129**, 823 (2007).
3. I. Albert *et al.*, *Nature* **446**, 572 (2007).
4. M. F. Dion *et al.*, *Science* **315**, 1405 (2007).
5. R. B. Deal, J. G. Henikoff, S. Henikoff, *Science* **328**, 1161 (2010).
6. A. Rufiange, P. E. Jacques, W. Bhat, F. Robert, A. Nourani, *Mol. Cell* **27**, 393 (2007).
7. T. Kaplan *et al.*, *PLoS Genet.* **4**, e1000270 (2008).
8. W. Xie *et al.*, *Mol. Cell* **33**, 417 (2009).
9. K. A. Lo *et al.*, *PLoS ONE* **6**, e19778 (2011).
10. S. Watanabe *et al.*, *Biochim. Biophys. Acta* **1799**, 480 (2010).
11. H. Neumann *et al.*, *Mol. Cell* **36**, 153 (2009).
12. H. Zhang, D. N. Roberts, B. R. Cairns, *Cell* **123**, 219 (2005).
13. N. J. Krogan *et al.*, *Mol. Cell* **12**, 1565 (2003).
14. G. Mizuguchi *et al.*, *Science* **303**, 343 (2004).
15. E. Luk *et al.*, *Cell* **143**, 725 (2010).
16. M. Papamichos-Chronakis, S. Watanabe, O. J. Rando, C. L. Peterson, *Cell* **144**, 200 (2011).
17. W. H. Wu *et al.*, *Nat. Struct. Mol. Biol.* **12**, 1064 (2005).
18. I. Celic *et al.*, *Curr. Biol.* **16**, 1280 (2006).
19. N. L. Maas, K. M. Miller, L. G. DeFazio, D. P. Toczyski, *Mol. Cell* **23**, 109 (2006).
20. R. T. Koerber, H. S. Rhee, C. Jiang, B. F. Pugh, *Mol. Cell* **35**, 889 (2009).
21. K. J. Pollard, C. L. Peterson, *Bioessays* **20**, 771 (1998).
22. T. Kusch *et al.*, *Science* **306**, 2084 (2004).
23. Y. Cai *et al.*, *J. Biol. Chem.* **280**, 13665 (2005).

Acknowledgments: We thank P. D. Kaufman (University of Massachusetts Medical School) for the gift of purified Rtt109/Vps75. We apologize to colleagues whose work we could not cite due to space constraints. This work was supported by grants from the NIH to C.L.P. (RO1 GM49650) and to O.J.R. (R01 GM079205). Chip-Seq data sets have been assigned the Gene Expression Omnibus accession no. GSE43935.

Supplementary Materials

www.sciencemag.org/cgi/content/full/340/6129/195/DC1
Materials and Methods
Figs. S1 to S15
References (*24*–*31*)

5 September 2012; accepted 20 February 2013
10.1126/science.1229758

Latency-Associated Degradation of the MRP1 Drug Transporter During Latent Human Cytomegalovirus Infection

Michael P. Weekes,[1]* Shireen Y. L. Tan,[1]* Emma Poole,[2]* Suzanne Talbot,[1]* Robin Antrobus,[1] Duncan L. Smith,[3] Christina Montag,[4] Steven P. Gygi,[5] John H. Sinclair,[2] Paul J. Lehner[1]†

The reactivation of latent human cytomegalovirus (HCMV) infection after transplantation is associated with high morbidity and mortality. In vivo, myeloid cells and their progenitors are an important site of HCMV latency, whose establishment and/or maintenance require expression of the viral transcript UL138. Using stable isotope labeling by amino acids in cell culture–based mass spectrometry, we found a dramatic UL138-mediated loss of cell surface multidrug resistance–associated protein-1 (MRP1) and the reduction of substrate export by this transporter. Latency-associated loss of MRP1 and accumulation of the cytotoxic drug vincristine, an MRP1 substrate, depleted virus from naturally latent CD14$^+$ and CD34$^+$ progenitors, all of which are in vivo sites of latency. The UL138-mediated loss of MRP1 provides a marker for detecting latent HCMV infection and a therapeutic target for eliminating latently infected cells before transplantation.

Human cytomegalovirus (HCMV) is a ubiquitous beta-herpesvirus that infects 60 to 90% of individuals (*1*). After primary infection, HCMV establishes a latent infection under the control of a healthy immune system. Reactivation from viral latency to productive infection causes serious disease in immunocompromised individuals, such as transplant recipients and AIDS patients (*1*, *2*).

Cells of the myeloid lineage, such as CD34$^+$ bone marrow progenitors and CD14$^+$ monocytes, are sites of latent HCMV infection (*3*–*5*). The viral genome persists in these cells with little gene expression and no detectable virus production (*6*, *7*). Reactivation from latency occurs upon myeloid differentiation, resulting in chromatin-mediated activation of the lytic gene expression cascade, viral DNA replication, and the production of infectious virions (*8*). Latent viral infection is thus required for viral persistence. Establishing how latency is maintained and how latently infected cells avoid immune recognition is crucial to understanding how HCMV persists in vivo. Furthermore, the elimination of latently infected cells is a key target in preventing recurrent HCMV infection in immunocompromised individuals.

A limited number of viral transcripts have been identified during natural latency in myeloid cells (*6*, *7*) and include UL138 (*9*, *10*), which encodes a 21-kD transmembrane Golgi-associated protein (*10*). UL138 is expressed with early-late kinetics during productive HCMV infection (*10*) but is also required for efficient latent carriage in vitro (*9*, *10*). The expression of UL138 during lytic infection results in increased tumor necrosis factor receptor 1 (TNFR1) cell surface expression (*11*, *12*), but little is known about UL138 during latency.

To address how UL138 affects host cell surface receptor expression during latent HCMV infection, we used plasma membrane profiling (PMP) (*13*), a proteomic technique that employs stable isotope labeling by amino acids in cell culture–based differential analysis to compare the expression of plasma membrane (PM) proteins in the presence and absence of UL138 in undifferentiated myeloid cells. Of the 592 PM proteins isolated from the monocytic cell line (THP-1), only 3 were reproducibly affected more than twofold (Fig. 1A and tables S1 and S2). Most notable was multidrug resistance–associated protein-1 (MRP1) (down-regulated 6.7- to 10.3-fold in three independent experiments), whereas Notch-ligand Delta-like protein 1 (DLL1) was down-regulated 2.1- to 2.6-fold. As expected, cell surface expression of TNFR1 increased (2.4- to 2.8-fold) (*11*, *12*).

These cell surface changes were confirmed by cell surface flow cytometry (DLL-1, TNFR1, and CD36) or intracellular flow cytometry (MRP1), whereas expression of the control protein (CCR7) was unaffected (Fig. 1B). UL138 down-regulated MRP1 in all four cell lines tested, including fibroblasts (Fig. 1C), HL60-ADR cells, a promyelocytic leukemia cell line that overexpresses MRP1 (*14*), and HeLa cells (fig. S1).

We focused on MRP1, the most dramatically down-regulated protein. In the presence of UL138, not only did MRP1 cell surface expression decrease but the protein was undetectable (Fig. 1, C and D). UL138 expression is not restricted to latent HCMV infection, is detected 6 hours after lytic infection, and accumulates over 48 hours (*10*). We analyzed the temporal

[1]Cambridge Institute for Medical Research, University of Cambridge, Hills Road, Cambridge CB2 0XY, UK. [2]Department of Medicine, University of Cambridge Clinical School, Addenbrookes Hospital, Hills Road, Cambridge CB2 2QQ, UK. [3]Paterson Institute for Cancer Research, University of Manchester, Wilmslow Road, Withington, Manchester M20 4BX, UK. [4]Laboratory for Molecular Biology, Children's Hospital, Charite Universitatsmedizin Berlin, Ziegelstrasse 5-9, D-10117 Berlin, Germany. [5]Department of Cell Biology, Harvard Medical School, 240 Longwood Avenue, Boston, MA 02115, USA.

*These authors contributed equally to this work.
†Corresponding author. E-mail: pjl30@cam.ac.uk